

Surface Quasi-Elastic Light Scattering From Spread Monolayers of a Poly(methyl methacrylate)–Poly(ethylene oxide) Block Copolymer

R. W. Richards,* B. R. Rochford, and M. R. Taylor

*Interdisciplinary Research Centre in Polymer Science and Technology,
University of Durham, Durham, DH1 3LE United Kingdom*

Received June 16, 1995; Revised Manuscript Received November 6, 1995

ABSTRACT: A linear diblock copolymer of poly(methyl methacrylate) and poly(ethylene oxide), with a mole ratio of methyl methacrylate to ethylene oxide units of 1:1, has been spread at the air–water interface. The surface visco-elastic parameters of this spread film, surface tension, γ_0 , transverse surface shear viscosity, γ' , dilational modulus, ϵ_0 , and dilational viscosity, ϵ' , have been determined using surface quasi-elastic light scattering. For a fixed value of the scattering vector parallel to the water surface, the surface visco-elastic parameters have been determined as a function of surface concentration of block copolymer. From the surface tension and transverse shear viscosity and using a simple Maxwell fluid model of the spread polymer, a relaxation time has been obtained which, from its concentration dependence at fixed angle of incidence for the incident light beam, suggests only a single relaxational process. Use of dilational parameters produces relaxation times of the same order which suggests that the same *molecular* process is involved in the relaxation process. For a fixed surface concentration of block copolymer the frequency dependence of the surface visco-elastic parameters has been investigated by selecting different scattering vectors. A capillary wave frequency from circa $1 \times 10^4 \text{ s}^{-1}$ to $2 \times 10^5 \text{ s}^{-1}$ has been explored here. A Maxwell model can be fitted to these data to provide a single relaxation time but the value is considerably different from that obtained using concentration dependent data at a single scattering vector. A Cole–Cole plot of these frequency dependent surface visco-elastic parameters clearly shows that a single relaxation time cannot prevail. A distribution in relaxation times is evident with the distribution apparently skewed to the high frequency side of the spectrum, but the frequency range we are able to explore is too limited to be able to define any parameters of this distribution.

Introduction

Polymers at fluid–fluid and fluid–solid interfaces have been of interest for many years with much of the attention being focused on the arrangement of polymers at such interfaces.¹ Typically, the segment density profile normal to the interface is sought either theoretically or via various experimental methods. A quantitative description of this organization together with an appreciation of the controlling factors is clearly of relevance to steric stabilization of colloids and the structural aspects relating to emulsion stability. A particular focus of attention has been the formation of polymer “brush” layers either at the solid–liquid interface or at the surface of a solid polymer film.^{2–4} In the majority of the work reported thus far fluid–solid interfaces constitute the majority of systems.^{5–7} polymers at fluid–fluid interfaces have been much less discussed.⁸ Of the work that has been reported, the majority discusses polymers at the air–water interface with organization being the main aspect examined.^{9–11} However, at such fluid interfaces there are also dynamic properties to be considered since the polymer layer will be continually perturbed by thermally driven random surface fluctuations, the capillary waves.

Although the fundamentals of such waves on liquid surfaces have been known for many years,¹² it is only in recent times that the influence of spread molecular films on the capillary waves has been expounded.^{13,14} Due to cohesion between molecules in the spread layer, extension of the film by a perturbing transverse capillary wave is resisted and the wave is damped. It has also been pointed out that there exists a coupling (albeit

weak) between these transverse waves and the longitudinal waves which produce a dilation and compression of the surface film.¹⁵ Consequently, observation of the effects of spread molecular films on the capillary wave frequency and damping can, in principle, provide transverse and dilational dynamic properties of the spread film. Goodrich^{16,17} postulated that the surface tension (γ) and dilational modulus (ϵ) obtained from such dynamic (frequency dependent) properties are visco-elastic parameters. Hence, these two parameters are complex quantities in which the imaginary frequency dependent contribution contains the relevant surface viscosities of the spread film.

The capillary wave amplitude is small (rms amplitude $\sim 2 \text{ \AA}$) but they are efficient scatterers of light, and the temporal evolution of the scattered light relates directly to the surface visco-elastic parameters of the spread molecular film. Essential features of the apparatus needed to collect this surface quasi-elastically scattered light were outlined by Hård and Neuman.¹⁸ Analysis of the scattered light intensity frequency distribution (the power spectrum) or its time dependence (the correlation function) requires a dispersion equation for the capillary waves when a molecular film is present. A useful expression for this purpose was provided by Langevin et al.¹⁹ and whatever method is used to collect the scattered light (i.e. power spectrum or correlation function), this equation forms the kernel of most analysis procedures. Surface quasi-elastic light scattering (SQELS) has been used to investigate a range of low molecular weight compounds either spread as films at the air–water interface or as a surface excess in surfactant solutions, additionally there has been considerable activity in the area of biological membranes or their models.^{20–25}

* To whom correspondence should be addressed.

† Abstract published in *Advance ACS Abstracts*, February 15, 1996.

SQELS studies of spread polymer films are much fewer in number. Early results on spread films of poly(methyl methacrylate) and polyvinyl acetate were reported by Langevin,²⁶ but here the attention was focused on the theory of the power spectrum. Yu and co-workers repeated this work and extended the range of polymers to include polyethers as well as a low molecular weight block copolymer of poly(ethylene oxide) and styrene at the air–water interface.^{27–29} In all of this work the power spectra were fitted by simple Lorentzian functions to extract the surface visco-elastic parameters. It has been shown that the power spectrum is actually a skewed Lorentzian^{30,31} and this needs to be taken into account. Furthermore, in some cases in the analysis of the power spectrum it has been assumed that the transverse shear viscosity is zero. Ignoring this factor may also bias the results obtained. Lastly, apart from one recent study of a block copolymer at the toluene–water interface,³² the range of momentum transfer (scattering angle) and hence capillary wave frequency (see below) has been limited, and thus an examination of phenomenological models was prevented. Moreover, in all the cases mentioned, nothing was known about the surface organization of the spread polymer at the interface although in some cases deductions about this aspect were attempted from the SQELS data. In an earlier paper we discussed some SQELS data obtained for poly(methyl methacrylate) at the air–water interface for which the surface organization was known from neutron reflectometry data.⁹ However, a full SQELS study was not undertaken at that time. We report here on a SQELS study of a linear diblock copolymer of poly(methyl methacrylate) (PMMA) and poly(ethylene oxide) (PEO). This copolymer has also been fully investigated by neutron reflectometry,^{33,34} and hence the surface visco-elastic properties may be related to the surface organization of the block copolymer. Following a precis of the relevant capillary wave theory and the background to the analysis of the SQELS data, a description of our experimental procedure is given. Data of two main types are then presented; firstly for a fixed wavenumber (q), the surface concentration dependencies of the visco-elastic parameters are presented. Secondly for one fixed surface concentration of block copolymer, the variation of the surface visco-elastic parameters with q (and hence capillary wave frequency) is set out. These data are then discussed using phenomenological models of the visco-elastic properties with the aim of extracting relaxation times for the spread films. The limits to such models are discussed, and we attempt a molecular explanation using the structural information from neutron reflectometry before presenting some general conclusions.

Theory

The surface of a liquid is continually roughened by random thermal fluctuations, and both transverse and longitudinal fluctuations are evident in addition to other possible modes. Of these two fluctuations only the transverse or capillary modes scatter light with sufficient intensity to be detected. There is sufficient coupling of these transverse modes with the longitudinal or dilational modes for dilational parameters to be extracted under favorable circumstances. We provide here a precis of the theoretical basis of surface quasi-elastic light scattering and an outline of how the relevant surface visco-elastic parameters can be extracted from the data. Fuller descriptions of the theoretical basis and the data analysis methods have been

presented elsewhere.^{20,35,36} Capillary fluctuations or waves are described by the displacement of the fluid surface from its equilibrium plane by the equation

$$d(r, t) = d_0 \exp i(qx + \omega t) \quad (1)$$

Where q is the surface wave number of the capillary wave which has a frequency ω and propagates in the x direction. The wavenumber is related to the wavelength, Λ , of the capillary wave by the relation

$$q = 2\pi/\Lambda \quad (2)$$

The frequency is a complex quantity which describes the time evolution of the surface due to fluctuations of frequency ω_0 which are subject to a decay process with a damping constant Γ

$$\omega = \omega_0 + i\Gamma \quad (3)$$

Capillary waves are dispersive and the dispersion relation between their frequency and wave number, q , for a fluid interface covered by a surface film is given by¹⁹

$$D(\omega) = [\epsilon q^2 + i\omega\eta(q + m)] [\gamma q^2 + i\omega\eta(q + m) - \omega^2 \rho / q] - [i\omega\eta(q - m)]^2 = 0 \quad (4)$$

where ϵ is the dilational modulus and γ the surface tension (or transverse modulus) of the surface film, η the viscosity, and ρ the density of the bulk liquid. In eq 4,

$$m = \sqrt{q^2 + i\omega\rho/\eta} \quad \text{for } \text{Re}(m) > 0 \quad (5)$$

The surface tension and dilational modulus in the most general case should be described as visco-elastic parameters due to additional energy dissipation processes taking place in the surface film as it relaxes to its equilibrium position after a perturbation; hence

$$\gamma = \gamma_0 + i\omega\gamma' \quad (6)$$

$$\epsilon = \epsilon_0 + i\omega\epsilon' \quad (7)$$

Where γ' is the transverse shear viscosity and ϵ' the dilational surface viscosity. The nature of these two parameters is not clear, but Goodrich¹⁷ has viewed them as surface excess properties due to inhomogeneities in the surface region. Capillary waves scatter light, and the power spectrum of this scattered light ($P(\omega)$) depends on the values of γ and ϵ .¹⁹

$$P(\omega) = -(k_B T / \pi \omega) \text{Im} \left[\frac{i\omega\eta(q + m) + \epsilon q^2}{D(\omega)} \right] \quad (8)$$

The influence of γ_0 , and γ' on $P(\omega)$ is shown in Figure 1. Fourier transforming the power spectrum gives the *field* autocorrelation function and the results of Fourier transforming such power spectra are shown in Figure 2.

We stressed above that it is the field autocorrelation function that is obtained because conventional homodyne quasi-elastic light scattering from bulk solutions utilizes the *intensity* correlation function. In surface quasi-elastic light scattering, to ensure that only the field correlation function is measured, a heterodyne technique is used. The correlation function produced has a beat pattern due to the slightly different frequen-

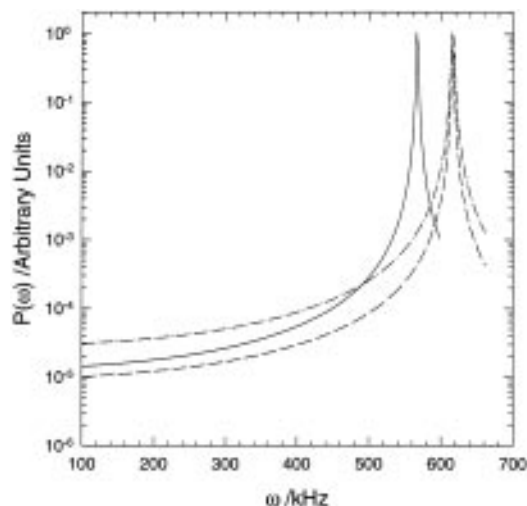


Figure 1. Power spectra calculated from eq 8: (a) —, $\gamma_0 = 55$ mN m $^{-1}$; $\gamma' = 3 \times 10^{-5}$ mN s m $^{-1}$; $\epsilon_0 = 0$ mN m $^{-1}$; $\epsilon' = 0$ mN s m $^{-1}$. (b) ---, $\gamma_0 = 65$ mN m $^{-1}$; $\gamma' = 3 \times 10^{-5}$ mN s m $^{-1}$; $\epsilon_0 = 0$ mN m $^{-1}$; $\epsilon' = 0$ mN s m $^{-1}$. (c) - · -, $\gamma_0 = 65$ mN m $^{-1}$; $\gamma' = 3 \times 10^{-4}$ mN s m $^{-1}$; $\epsilon_0 = 0$ mN m $^{-1}$; $\epsilon' = 0$ mN s m $^{-1}$.

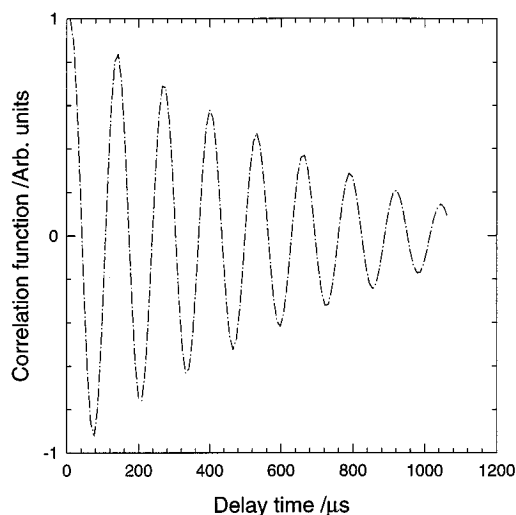


Figure 2. Autocorrelation function obtained from the power spectra of Figure 1c.

cies of the reference beam and the scattered light. The heterodyne intensity correlation function obtained is given by³⁷

$$G_H(\tau) \propto (I_s + I_r)^2 + 2I_s I_r g^1(\tau) + I_s^2 (g^2(\tau) - 1) \quad (9)$$

where I_s and I_r are the intensities of the scattered and reference light beams, respectively, $g^1(\tau)$ is the field autocorrelation function, $g^2(\tau)$ is the intensity correlation function, both of which are normalized and τ is the delay time. The scattered intensity is weak; consequently, the homodyne contribution (the last term on the right hand side of eq 9) to $G_H(\tau)$ is very small and when $I_r/I_s > \sim 30$ it is negligible and thus

$$G_H(\tau) \propto (I_s + I_r)^2 + 2I_s I_r g^1(\tau) \quad (10)$$

Earnshaw and co-workers³⁶ have developed a method of analyzing the field correlation functions to provide the four surface visco-elastic parameters. This direct method consists of calculating the power spectrum from estimates of γ_0 , γ' , ϵ_0 , and ϵ' using eq 8, the calculated spectrum is then numerically fast Fourier transformed and the sum of the square of the difference between

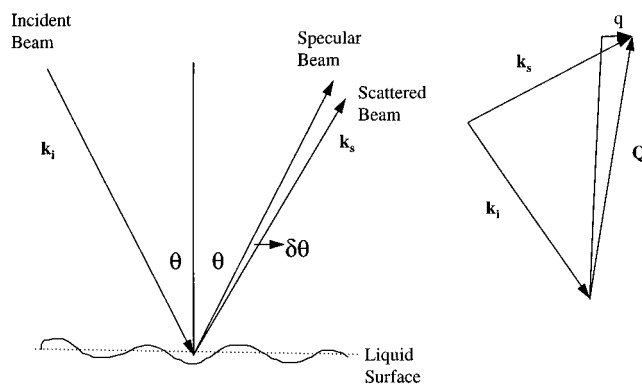


Figure 3. Incident and scattered wave vectors and definition of the scattering vector q in the plane of the water surface.

calculated and experimental correlation function is minimized by iterating around this loop using the surface visco-elastic parameters as adjustable variables in the fitting procedure. In practical terms the heterodyne correlation function is obtained by focusing the weak reference beams obtained by passing a laser beam through a transmission grating and the main beam on to the same point on the liquid surface. Each reference beam is incident on the surface at a slightly different angle and thus probes a different capillary wavelength since the wave vector $q = 2\pi/\Lambda$. On reflection from the liquid surface the reference beam and specularly reflected main beam diverge at a small angle, $\delta\theta$, which allows the reference beam and the scattered light to be focused on the photomultiplier well away from the main beam. The situation is schematically shown in Figure 3 and the wave vector parallel to the liquid surface is:

$$q = \frac{4\pi}{\lambda} \sin\left(\frac{\delta\theta}{2}\right) \cos \theta \quad (11)$$

Given the surface visco-elastic properties of a fluid surface, the value of q is highly relevant to the ease of observation of the influence of dilational parameters and transverse shear viscosity. To obtain ϵ_0 and ϵ' , the dilational modes need to be well coupled to the transverse modes and this translates to the conditions, $\epsilon/\gamma < 0.5$ and $\epsilon'q/2\eta < 10$, this indicates that small q values are required. On the other hand, γ' values are more accurately determined using high q values.

Experimental Section

Copolymer Preparation. The diblock copolymer of methyl methacrylate (MMA) and ethylene oxide (EO) was synthesized under high vacuum by anionic polymerization. The polymerization solvent was tetrahydrofuran (THF) and a solution of methyl methacrylate in THF was cooled in a dry ice and acetone bath before a known volume of initiator solution was injected ((diphenylmethyl)potassium in THF). The polymerization was allowed to continue for circa 2 h before the required mass of ethylene oxide was distilled into the reaction flask. Flask and contents were then allowed to warm to room temperature overnight, after which they were kept at 348 K for 1 week. After cooling, a small amount of glacial acetic acid was added as terminating agent. The solution of polymer was poured into well stirred hexane, filtered off, washed and dried at 343 K to constant weight. Molecular weights obtained by size exclusion chromatography using chloroform as solvent and polystyrene calibration and tacticity from ^{13}C NMR are reported in Table 1. ^1H NMR gave the composition of the copolymer as 1:1 on a molar basis of MMA and EO segments.

Surface Pressure Isotherm. A NIMA (Warwick Science Park, Coventry, UK) surface film balance was used to deter-

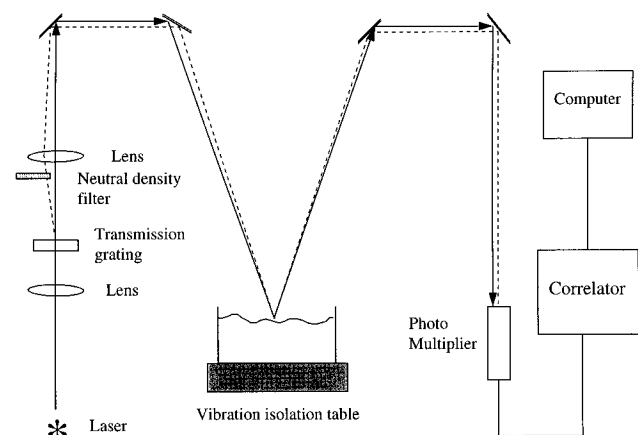


Figure 4. Schematic arrangement of optical components for surface quasi-elastic light scattering.

Table 1. Characterization Data of the Block Copolymer

polymer	M_w , g mol ⁻¹	M_w/M_n	diad content from NMR		
			isotactic	heterotactic	syndiotactic
PMMA	38 000	1.3			
copolymer	62 700	1.4	0.065	0.545	0.39

mine the surface pressure isotherm of the block copolymer. A solution of the copolymer in chloroform was made such that the concentration was circa 1 mg mL⁻¹ but accurately known. A known volume (~30 μ L) of this solution was spread on to the previously cleaned water surface in the trough of the film balance. After allowing 15 min for complete evaporation of the spreading solvent, the initial area of 900 cm² was reduced by closing the barriers at a constant rate of 30 cm² min⁻¹. The change in surface pressure was continuously recorded via a Wilhelmy plate and transducer connected to a computer.

Surface Quasi-Elastic Light Scattering. Figure 4 shows a schematic sketch of the components of the SQELS apparatus, and this is little different from equipment used by others. In our case the laser was a vertically polarized He Ne laser with a power of 35mW; the transmission grating was obtained from Datasights Ltd (Enfield, Middlesex, UK) and was composed of 10 μ m wide opaque lines separated from each other by a center-to-center distance of 100 μ m. The neutral density filter through which half of the reference beams were passed was a Kodak Wratten gel filter and was chosen to give a suitable I_r/I_s ratio without "flooding" the photomultiplier tube. The output from the photomultiplier tube was passed to a Malvern K7025 correlator with 128 delay channels arranged serially; an oscilloscope connected to the correlator provided a live display of the correlation function. By selecting different reference beams, a range of wave vectors, q , parallel to the water surface were investigated. Values of q from circa 300 to 910 cm⁻¹ have been investigated here.

The water surface was contained in the trough of the NIMA film balance which was placed on an active vibration isolation table (JRS, Affoltern, Switzerland). All of the optical components and the active vibration isolation table were mounted on a heavy optical table. These measures were generally sufficient to remove adventitious high frequency vibrations, but there still remained "building" vibrations resulting from normal activity, and these appear as a low frequency oscillation causing the correlation functions to droop at long delay times. These are accounted for in the data analysis procedure, but any correlation functions where droop was observed in the live display were discarded.

For each reference beam the associated value of q was obtained by collecting the SQELS correlation function for light scattered from the surface of clean water. From the values of the frequency (ω_0) and damping constant (Γ) obtained by fitting a modified cosine function to the data (vide infra) the value of q can be calculated approximately using the relations

$$\omega_0^2 = \gamma_0 q^3 / \rho \quad (12)$$

$$\Gamma = 2\eta q^2 / \rho \quad (13)$$

where γ_0 , ρ , and η are the surface tension, density, and viscosity of pure water at the temperature of measurement. There are correction terms to both of these equations which become more important as q increases particularly for the damping coefficient. Corrections to the expression for the frequency were essentially negligible over the q range accessible to us and hence we used eq 12 exclusively to calculate q . Additionally, we compared our ω_0 and q values with those reported by Earnshaw,²³ we obtained complete agreement with his values.

SQELS Data Analysis. Field auto correlation functions were analyzed by two methods. The most straightforward analysis procedure was a nonlinear least squares fit of a damped cosine function to provide the frequency and damping constant of the capillary waves. The simple damped cosine function has been adapted to account for various additional factors; these factors include³⁸ (1) Instrumental broadening, (2) Adventitious building vibrations ("droop"), and (3) Fast processes and after pulsing in the photomultiplier.

The form of the cosine function fitted to the normalized correlation function is

$$g(\tau) = B - D\tau^2 + A_f \exp(-\Gamma_f \tau) + A \exp(-\beta^2 \tau^2 / 4) \times \exp(-\Gamma \tau) \cos(\omega_0 \tau + \phi) \quad (14)$$

The droop is accounted for by the term $(B - D\tau^2)$, fast processes are described by $A_f \exp(-\Gamma_f \tau)$ where A_f is the amplitude of the process which has a decay constant Γ_f . Additionally, to overcome possible afterpulsing we usually disregard the first one or two delay channels in the subsequent fitting process. Due to the finite size of the laser beam and the solid angle subtended at the surface by the detector, the wavenumber range of capillary waves on the surface illuminated is finite; this broadened resolution is described by the $\exp(-\beta^2 \tau^2 / 4)$ where β is the standard deviation of the Gaussian resolution function. This standard deviation was kept as a free parameter in the fitting process. Although the power spectrum of the light scattered by a liquid surface is often approximated to a Lorentzian function, we have already noted that it is slightly skewed. Therefore to include this skewing a phase term, ϕ , is incorporated into the fitting function. The damped cosine function equation (eq 14) was incorporated into a FORTRAN program, and the quality of the fit and the nature of the residuals are shown in Figure 5.

For evaluation of the four surface visco-elastic parameters, the direct spectral fitting method was used.³⁶ The core equation is similar to eq 14 except that the damped cosine function was replaced by the Fourier transform of the power spectrum (eq 8). The use of this method was pioneered by Earnshaw and its application; limitations and justification have been exhaustively discussed.^{30,35,36} In its use to obtain the parameters set out here, care was taken to repeat the spectral fitting using different starting points to ensure that global minima were found when the final fitted parameters were produced. Figure 6 shows the quality of fit obtained to the heterodyne correlation functions and the residuals between fitted and experimental data points. For each concentration or q value, 10 correlation functions were collected and individually analyzed. The error bars on the points reflect the spread in values obtained from these 10 determinations.

Results

Figure 7 shows the static surface pressure isotherm (surface pressure as a function of surface concentration (Γ_s)) obtained for this block copolymer; some comments are appropriate here. In obtaining these data, the water surface is aspirated until barrier compression to the smallest area produces no change in surface pressure. At this point the barriers were opened to maximum area and the surface pressure set to zero. On deposition of the block copolymers a negative reading for surface

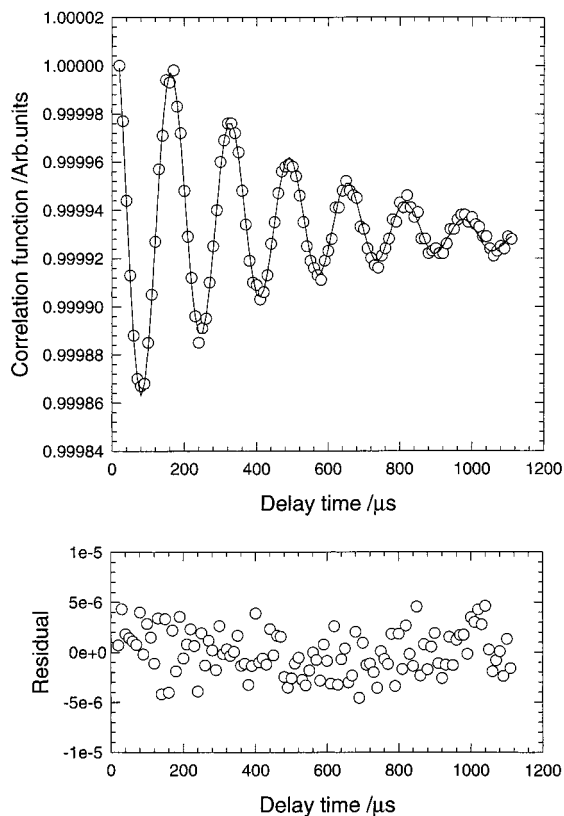


Figure 5. Typical fit (—) of damped cosine function (eq 14) to the correlation function obtained by SQELS. These data obtained at $q = 351 \text{ cm}^{-1}$ and for $\Gamma_s = 1.50 \text{ mg m}^{-2}$.

pressure was always obtained; considerable compression of the spread film was required before a positive surface pressure reading was obtained. This behavior has

always been observed by us when syndiotactic poly(methyl methacrylate) is present in the spread film in some form.³⁹ It is *not* observed when pure poly(ethylene oxide) homopolymer or isotactic poly(methyl methacrylate) are spread at the air–water interface; we return to this point when considering the SQELS results. The isotherm in Figure 7 displays characteristics of isotherms for both pure poly(ethylene oxide) apart from the large finite surface concentration required before any surface pressure is noted. Poly(ethylene oxide) spread monolayers have an asymptotic surface pressure of 10 mN m^{-1} ; the copolymer surface pressure exceeds this and has an asymptotic surface pressure of circa 35 mN m^{-1} which is characteristic of that observed for syndiotactic poly(methyl methacrylate).⁹

Surface Quasi-Elastic Light Scattering. For one selected wavenumber ($q = 351 \text{ cm}^{-1}$), correlation functions were obtained over the whole range of surface concentration explored in the static surface pressure isotherm. Figure 8 shows the dependence of capillary wave frequency and damping coefficient as a function of the surface concentration of block copolymer, at a temperature of 298 K . As surface concentration increases the frequency decreases and there are evident transition regions in the data. The damping constant shows a small initial decrease from that of water before a sharp increase is noted at a surface concentration of circa 0.5 mg m^{-2} . We point out here that the presence of the copolymer on the surface is observable to much lower concentrations in SQELS than in the static surface pressure isotherms. A rather ill defined maximum appears to be present in the damping constant at $\Gamma_s \approx 0.5 \text{ mg m}^{-2}$. Such maxima are predicted to occur when $\epsilon_0/\gamma_0 \approx 0.16$. The increase in the damping at a surface concentration of 0.5 mg m^{-2} could be due to a sharp increase in surface shear viscosity, γ' ; at this

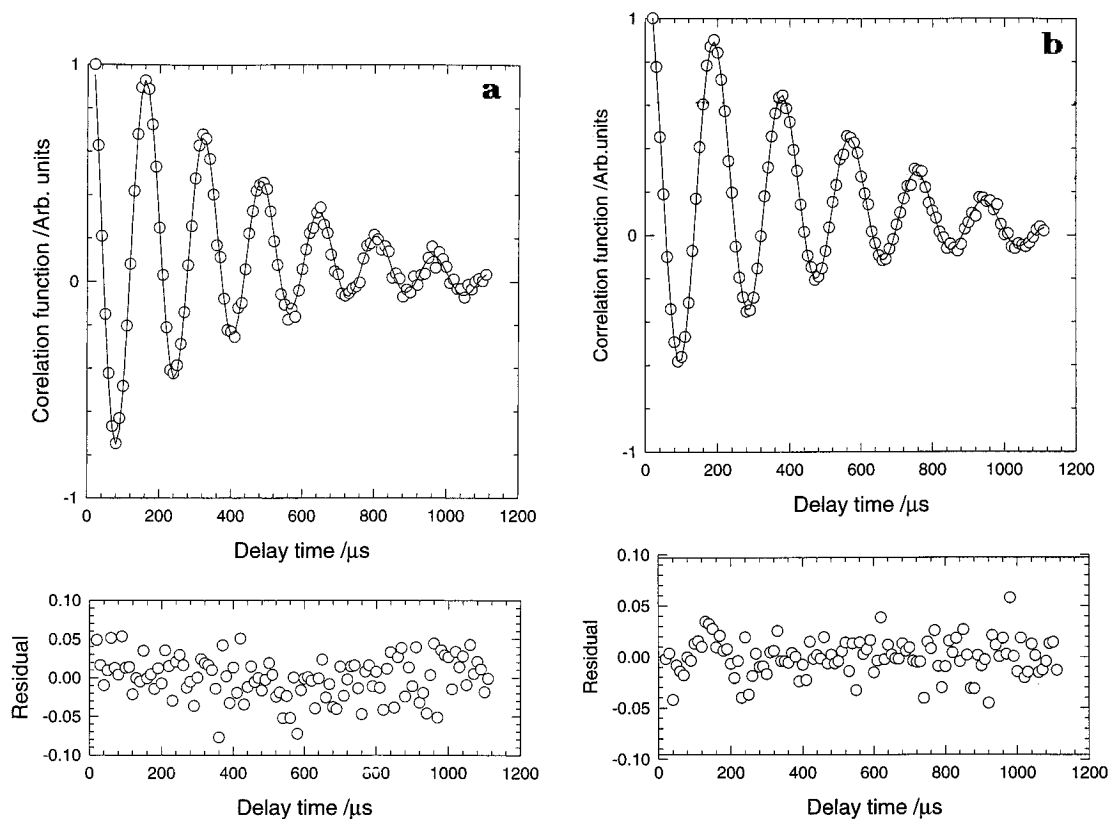


Figure 6. Typical fits (—) and residuals from the full spectral fitting to correlation function data. For both cases $q = 351 \text{ cm}^{-1}$, (a) $\Gamma_s = 1.50 \text{ mg m}^{-2}$, (b) $\Gamma_s = 2.50 \text{ mg m}^{-2}$.

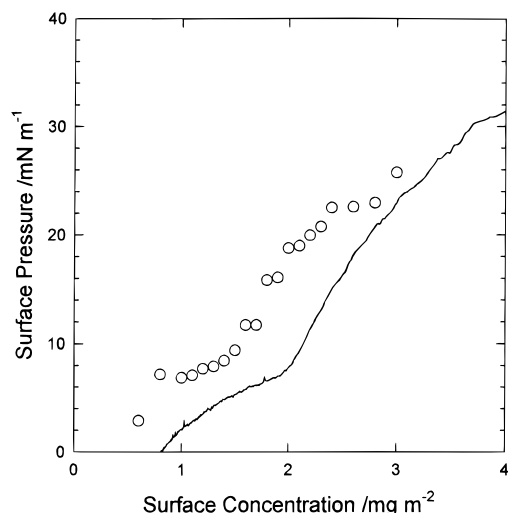


Figure 7. Classic surface pressure isotherm (solid line) obtained for the block copolymer at a temperature of 298 K. The points are the surface pressures obtained from SQELS values of the surface tension.

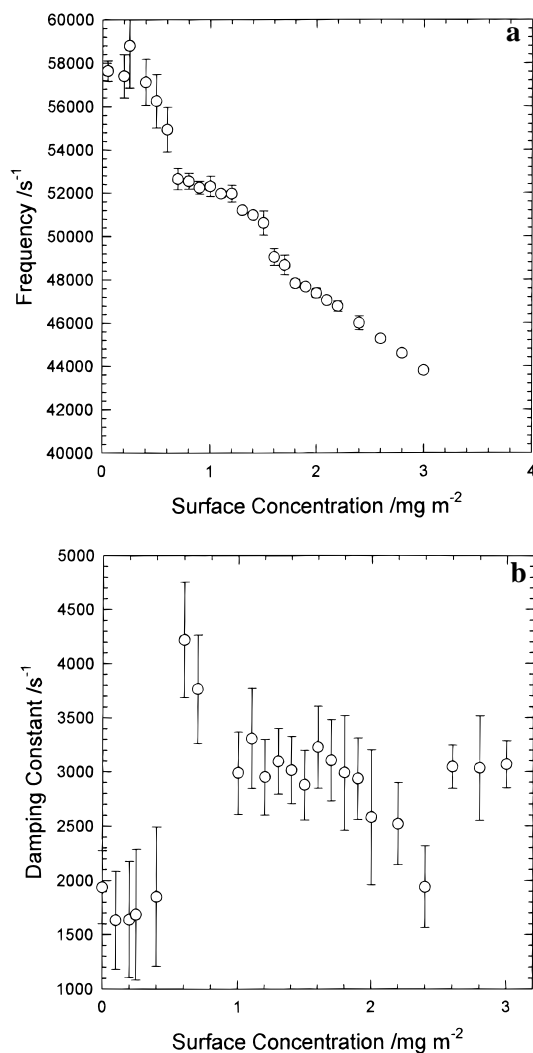


Figure 8. Dependence of (a) capillary wave frequency (ω_0) and (b) damping (Γ) as a function of block copolymer surface concentration (Γ_s) at $q = 351 \text{ cm}^{-1}$ and a temperature of 298 K. Where no error bars are apparent they are within the symbol.

concentration, the small decline in damping constant at higher concentrations is determined by the ϵ_0/γ_0 ratio as well as the change in surface viscosity. It is because

of this different influence that surface visco-elastic parameters have on capillary wave frequency and damping that a direct spectral fitting method becomes necessary to analyze the correlation functions.

Surface visco-elastic moduli obtained from spectral fitting to these same field correlation functions are shown in Figure 9. The surface tension starts at a value marginally higher than that of clean water and remains at this higher value until Γ_s reaches 0.6 mg m^{-2} where the SQELS-determined surface tension decreases and then continues to decrease as surface concentration increases. The transverse shear viscosity has a small finite value at very low surface concentrations which is approximately constant as surface concentration increases to circa 0.6 mg m^{-2} before undergoing an abrupt increase at a surface concentration circa 0.7 mg m^{-2} . A maximum in the surface viscosity is observed in the surface concentration region of 1.5 mg m^{-2} which coincides with the concentration range where the static surface pressure seems to be approaching a lower asymptotic value. Both dilational elastic modulus (ϵ_0) and dilational viscosity also show a maximum in this same region of surface concentration.

Figure 7 shows the static surface pressure obtained using the surface film balance and the surface pressure calculated from surface tension data obtained from SQELS, i.e. the difference between the surface tension of pure water and the SQELS surface tension data. The surface pressure isotherm derived from the SQELS data is qualitatively similar to the static surface pressure, but because of the concentration dependent frequency (i.e. ω_0) at which the SQELS measurements are obtained, the surface pressure is a *dynamic* value, and they are somewhat larger than the equilibrium ($\omega_0 = 0$) values obtained in the classical manner.

By selecting different reference beams, capillary waves of different wavenumber and frequency are observed. A study of the frequency dependence of the surface visco-elastic properties has been undertaken for the spread copolymer layer at 3.0 mg m^{-2} , i.e. approaching full compression. Figure 10 shows the dependence of each visco-elastic parameter on the capillary wave frequency. Surface tension increases to a plateau value as the frequency increases whereas the transverse shear viscosity decreases with increased capillary wave frequency. Both dilational modulus and dilational viscosity at this high surface concentration show a decrease as the capillary wave frequency increases, in particular the dilational viscosity rapidly drops to values which are essentially zero within the capabilities of our equipment.

Discussion

Phenomenological Models. The capillary waves subject the spread monolayer to an oscillatory stress and strain which are complex quantities, σ^* and γ^* , respectively, which are related via the complex shear modulus, G^* .^{40,41}

$$\sigma^* = G^* \gamma^* \quad (15)$$

In its turn the complex shear modulus is the sum of the storage and loss modulus of the spread polymer film

$$G^* = G'(\omega_0) + iG''(\omega_0) \quad (16)$$

where $G'(\omega_0)$ is the storage modulus at a frequency ω , and $G''(\omega_0)$ the corresponding loss modulus. For the quantities derived from SQELS data, the storage modu-

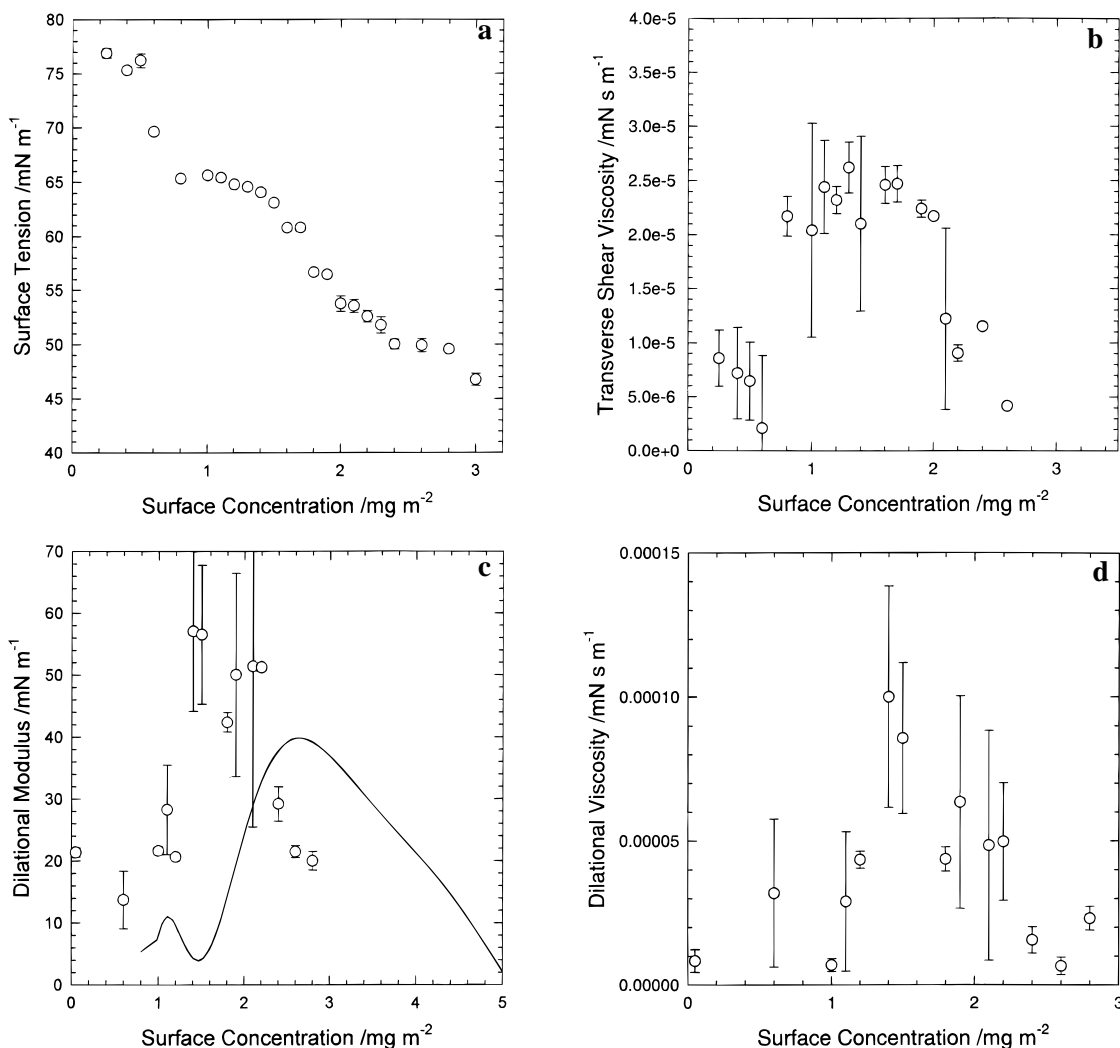


Figure 9. Concentration dependence of surface visco-elastic parameters obtained at $q = 351 \text{ cm}^{-1}$ and a temperature of 298 K: (a) surface tension, (b) transverse shear viscosity, (c) dilational modulus, (d) dilational viscosity. Solid line in c is the dilational modulus obtained from the classical surface pressure isotherm.

lus is identified with the surface tension (or dilational modulus) obtained at a particular q value and hence capillary wave frequency. The transverse shear viscosity (or dilational viscosity) relates to the loss modulus via

$$G''(\omega_0) = \gamma' \omega_0 \text{ (or } \epsilon' \omega_0) \quad (17)$$

On this basis we can attempt the application of simple phenomenological models to the surface visco-elastic parameters obtained for the spread copolymer film. These are generally described in terms of combinations of springs and dashpots, and although many such combinations could describe dynamic moduli data, discussions are generally restricted to two simple models, i.e. a Maxwell fluid and a Voigt solid. Simplifying these models yet further by assuming there is only one exponential relaxation process for the Maxwell fluid model then

$$G'(\omega) = G_e + G_i \frac{\omega_0^2 \tau^2}{1 + \omega_0^2 \tau^2} \quad (18)$$

$$G''(\omega) = G_i \omega_0 \tau / (1 + \omega_0^2 \tau^2) \quad (19)$$

where G_e is the modulus at infinite relaxation time (i.e.

$\omega_0 = 0$), which corresponds to the surface tension given by the surface pressure isotherm. The G_i term is the magnitude of the relaxation process. For a Voigt solid

$$G'(\omega) = G_i \quad (20)$$

$$G''(\omega) = G_i \omega \tau \quad (21)$$

Since both the surface tension and the transverse shear viscosity obtained by us are frequency dependent, we confine our attention to the Maxwell model only. Replacing $G'(\omega)$ by γ_0 , $G''(\omega)$ by $\omega_0 \gamma'$, and G_e by $\gamma(\omega_0 = 0)$ and rearranging eqs 18 and 19 we have

$$\tau = \frac{\gamma_0 - \gamma(\omega_0 = 0)}{\omega_0^2 \gamma'} \quad (22)$$

$$= - \frac{\Delta \pi}{\omega_0^2 \gamma'} \quad (23)$$

where $\Delta \pi = \pi(\omega_0) - \pi(\omega_0 = 0)$ with $\pi(\omega_0)$ the surface pressure obtained from the light-scattering (i.e. frequency dependent) surface tension, and $\pi(\omega_0 = 0)$ is the classical value obtained from conventional surface pressure isotherms. Consequently using the variation of ω_0 , γ_0 , and γ' with Γ_s , the relaxation time of the spread

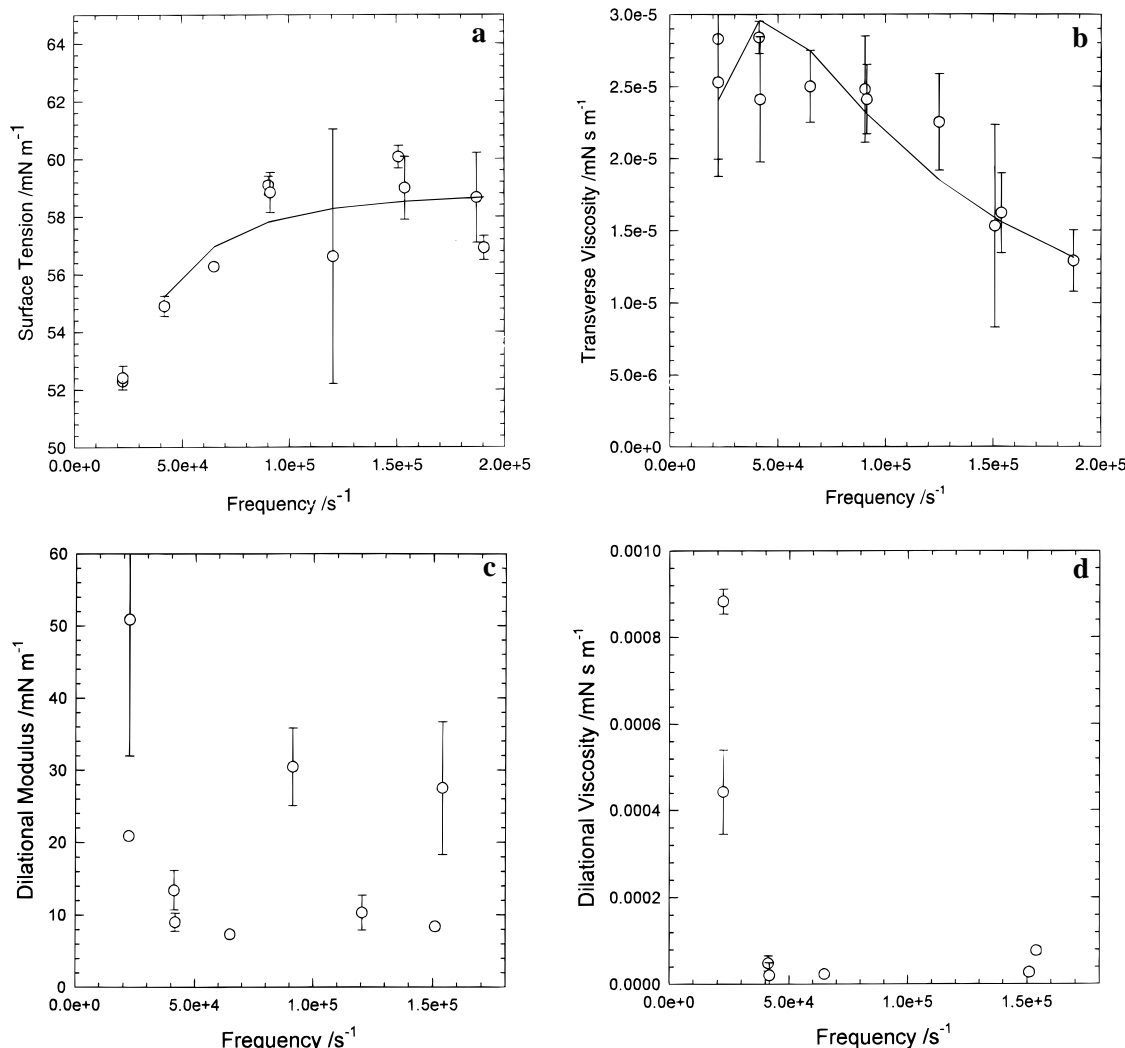


Figure 10. Frequency dependence of surface tension (a), transverse shear viscosity (b), dilational modulus (c), and dilational viscosity (d) at $\Gamma_s = 3.0 \text{ mg m}^{-2}$. Solid lines in a and b are fits of Maxwell model to the data.

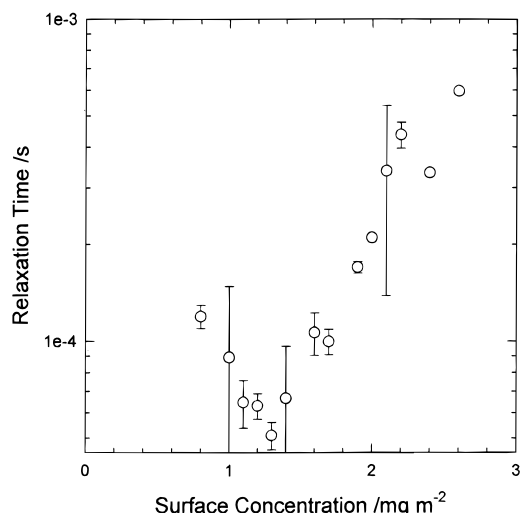


Figure 11. Relaxation time (τ) calculated from eq 22 as a function of surface concentration (Γ_s) for $q = 351 \text{ cm}^{-1}$.

copolymer film can be calculated at each Γ_s value. We are aware that this model may be a simplistic description of the surface hydrodynamics, but in view of the rather limited frequency range accessible (see below) we do not believe we are justified in applying more complicated models at this stage.

Surface Tension and Transverse Shear Viscosity. Relaxation times have been calculated using eq 23 for a q value of 351 cm^{-1} over the surface concentration range of circa 0.2 mg m^{-2} to 3.0 mg m^{-2} . These data are presented in the semilog plot of Figure 11, which indicates that the relaxation time increases exponentially with surface concentration of copolymer for $\Gamma_s \geq 1.2 \text{ mg m}^{-2}$. Over the range of surface concentrations for which relaxation times have been obtained, the relaxation times increase by 1 order of magnitude over the range of Γ_s investigated, values between $40 \mu\text{s}$ to $500 \mu\text{s}$ being observed. We note that the relaxation time increases with Γ_s over most of the concentration range, but there is clearly an initial decrease in τ . In separate experiments we have obtained the surface organization of this block copolymer using neutron reflectometry.^{33,34} The concentrations explored are much fewer than those discussed here, but it is clear that for a surface concentration above 1.5 mg m^{-2} the block copolymer is organized into two distinct layers. The PMMA block is mainly in the air phase but with some penetration of the subphase, the PEO block is totally immersed in the aqueous subphase. At a lower surface concentration of 0.7 mg m^{-2} the two blocks form a mixed homogeneous layer which contains a finite volume fraction of water. What we do not know is the precise surface concentration where this phase transition takes place; however, it is tempting to associate it with the surface concentra-

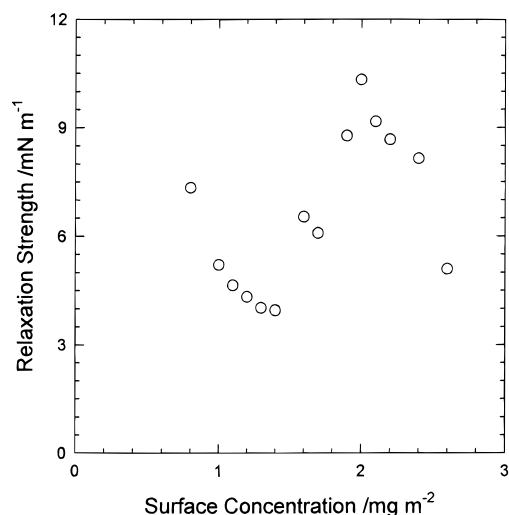


Figure 12. Relaxation strength, G_i , as a function of surface concentration.

tion where we observe a change in the relaxation time calculated from the combination of SQELS data and classical surface pressures. With these values of τ , the magnitude of the relaxation process can be calculated from eq 16 using γ' values to calculate loss moduli. Figure 12 shows G_i as a function of block copolymer surface concentration. All the values of the relaxation strength are between 4 to 10 mN m^{-1} , as Γ_s increases the relaxation strength appears to decrease before an increase is observed at circa 1.5 mg m^{-2} . Above 2 mg m^{-2} the relaxation strength again decreases.

The relaxation times obtained are very long compared to those that have been reported for spread films of low molecular weight materials at the air–water interface.⁴² Values of the relaxation time for this block copolymer are of the order of 2 orders of magnitude greater than comparable data for low molecular weight materials. This large difference is not unexpected given the large difference in surface pressure obtained from SQELS surface tension data compared to classical values of π that we observe for all the surface concentrations studied. Surface pressure differences from SQELS and classical data for small molecules are generally very small. Moreover this difference in surface pressure is approximately constant over this whole concentration range, a slight decrease being evident at higher values of surface concentration. Consequently, although γ' goes through a maximum at $\Gamma_s \sim 1.5 \text{ mg m}^{-2}$, and has rather small values for $\Gamma_s \sim 2.5 \text{ mg m}^{-2}$, we are still able to obtain values of τ and G_i . Furthermore, because the relaxation times are long, the variation of G_i over the range of Γ_s is very modest and G_i increases with Γ_s slightly because $\Delta\pi$ decreases slightly at larger values of Γ_s . From these values of G_i and τ , the frequency variation of $\Delta\pi$ and the transverse surface viscosity can be calculated assuming the Maxwell model is applicable. The calculated variation obtained for three different values of Γ_s is shown in Figure 13. At low q , which corresponds to low capillary wave frequency, a marked variation in $\Delta\pi$ and γ' values with surface concentration is observed. At higher frequencies it appears that the distinction between values of γ' for the different surface concentrations is much reduced. The frequency range accessible on our apparatus is from circa $2 \times 10^4 \text{ s}^{-1}$ to $2 \times 10^5 \text{ s}^{-1}$.

In addition to obtaining values for the relaxation time as a function of surface concentration at a fixed q value,

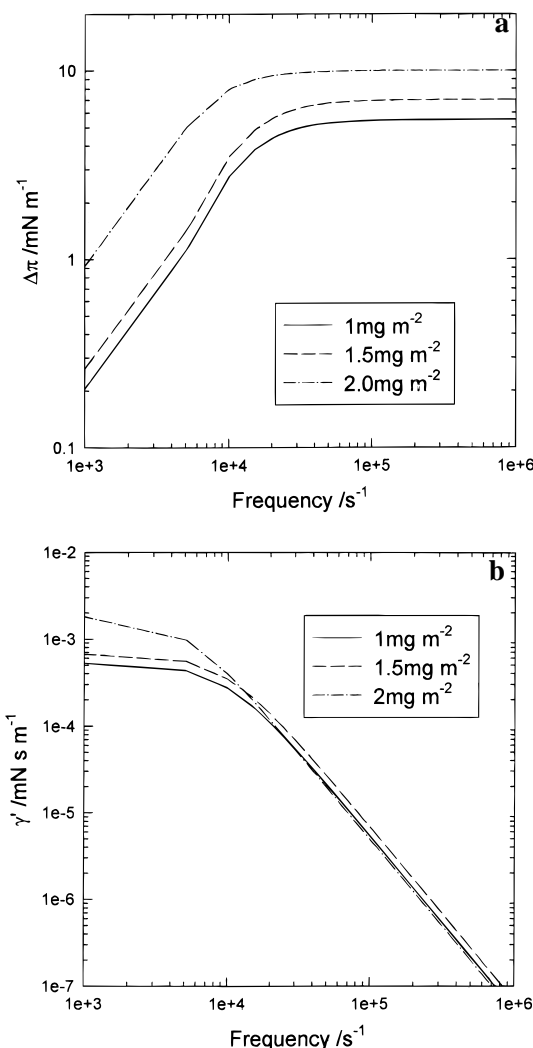


Figure 13. Frequency dependence of (a) $\Delta\pi \equiv G'(\omega_0) - G_e$ and (b) $\gamma' \equiv G''(\omega_0/\omega_0)$ calculated using a Maxwell model from the measured values of τ and G_i for three different surface concentrations of block copolymer.

eqs 18 and 19 can also be used to obtain relaxation times from the frequency dependence of γ_0 and γ' for a fixed concentration. Because of the implications of Figure 13 at higher frequency, we have used a high surface concentration in order to improve signal to noise ratio so that the surface visco-elastic parameters are obtainable with reduced error. Equation 18 was nonlinearly least squares fitted to the γ_0 data and γ' data obtained for $\Gamma_s = 3.0 \text{ mg m}^{-2}$ for a range of q values (and hence capillary wave frequencies), the results of this procedure are shown in Figures 10a and 10b and a relaxation time of $25.9 \mu\text{s}$ was obtained. The value of G_e obtained from this fit was 49.49 mN m^{-1} which is in excellent agreement with the surface tension of 48.95 mN m^{-1} obtained from the classical surface pressure isotherm. The relaxation strength obtained from the fit was 9.47 mN m^{-1} , which is in concordance with the values obtained from the surface concentration variation of G_i (Figure 12). The relaxation time obtained by this fitting procedure is sufficiently different from the values anticipated from the values of τ obtained from the concentration variation of γ_0 and γ' at $q = 351 \text{ cm}^{-1}$, to provoke further enquiry. Calculation of the relaxation time for each q value separately shows quite clearly that the relaxation times are dependent on the surface wave-number q . Hence the possibility arises that rather than a single exponential relaxation process being present,

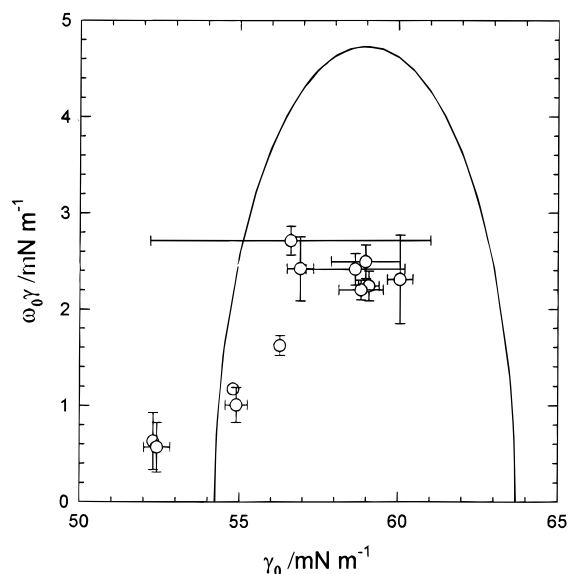


Figure 14. Cole-Cole plot of frequency dependence of transverse visco-elastic moduli.

a distribution of relaxation times exist and the relaxation mode sampled depends on the q value utilized. Some evidence for this is obtained when the loss modulus is plotted against the surface tension (storage modulus), Figure 14. This is equivalent to a Cole-Cole plot,⁴⁰ and if a single relaxation process is taking place, then the data should lie on a semicircle of radius $G_i/2$ whose origin is at $G_e + G_i/2$; the theoretical semicircle is shown as the solid line in Figure 14. Clearly from Figure 14 we have not been able to explore a sufficiently high frequency (i.e. q value) to define the complete range of surface tension predicted by the theoretical curve. Nonetheless it does appear that the data are skewed from the ideal semicircle as well as having magnitudes of $\omega_0\gamma'$ which are smaller than those predicted. These data suggest that the relaxation times obtained are frequency (and hence q) dependent and thus they should be treated as *apparent* values. The shape of the arc described by the current data is reminiscent of the skewed distribution of Davidson and Cole⁴³ for high frequency broadening. In these cases, the arc on the low frequency side approaches the abscissa along a straight line, the slope of which is related to the frequency at the maximum via a characteristic relaxation time. The absence of surface tension and transverse shear viscosity data at higher frequencies makes the application of this model to the data highly speculative, especially as we are unable to say with certainty that we have sampled the capillary wave frequency where the maximum value of the loss modulus is observed.

Dilational Surface Visco-Elastic Parameters.

We point out again here that dilational parameters, ϵ_0 , and ϵ' , have only an indirect influence on the capillary waves, and hence the accuracy of the evaluation of ϵ_0 and ϵ' must be carefully reviewed. Furthermore, the observation of ϵ_0 depends critically on the signal to noise ratio and the errors can become extremely large when the noise constitutes a finite proportion of the total signal. Added to this is the decreasing influence of ϵ_0 as the momentum transfer, q , parallel to the surface increases. Indeed for q values greater than circa 400 cm^{-1} for the present copolymer, ϵ' was either zero or indeterminate whereas ϵ_0 displayed rather wide fluctuations from q value to q value. Consequently we

discuss here only the variation of ϵ_0 with surface concentration at $q = 351 \text{ cm}^{-1}$. These data are plotted in Figure 9 where we also include the classical value of the dilational modulus ($\Gamma_s d\pi/d\Gamma_s$). This latter parameter was obtained by fitting a polynomial to the surface pressure isotherm data over the range for which π was positive. Over most of the range of Γ_s for which data are available, the SQELS-determined values exceed the classically determined values of ϵ_0 by an appreciable amount. To some extent this is expected because visco-elastic moduli are expected to increase with frequency. However, whereas the classical values of ϵ_0 show two maxima and a minimum, we cannot state that this is observed in the SQELS values of ϵ_0 due to the large error bars on some of the values. The surface dilational viscosity also goes through a maximum as does γ' in a region where $\Gamma_s \sim 1.5 \text{ mg m}^{-2}$. The values of ϵ' are modest when compared to those observed for low molecular weight monolayers. Relaxation times for each surface concentration have been calculated using ϵ' , ω_0 , and values of $\epsilon_0(\omega_0) - \epsilon_0(\omega_0 = 0)$ in eq 22 over the range of Γ_s where the SQELS values exceed the classical dilational modulus. No strong concentration dependence of the dilational relaxation time was noted, the average value obtained being $254 \pm 60 \mu\text{s}$. This average dilational relaxation time is of the same magnitude as the relaxation times obtained from the transverse shear viscosity and surface tension data for the same concentration range.

Molecular Basis. Although there are as yet no theories available for visco-elastic relaxations in spread polymer monolayers, we can attempt some molecular level description, albeit speculative. We are able to do this because we have insight into the structural arrangement of this block copolymer at the air-water interface from our separate neutron reflectometry experiments.³⁴ These data are only available for discrete values of Γ_s , but the use of selective deuterium labeling and the kinematic approximation clearly shows that a form of phase separation takes place when Γ_s is increased. Thus at $\Gamma_s = 0.6 \text{ mg m}^{-2}$, both MMA and EO are mixed together and occupy the same volume and there is little penetration by the aqueous subphase. When Γ_s is 1.6 mg m^{-2} , the MMA and EO parts of the block copolymer occupy different spatial volumes with the subphase being penetrated by the EO blocks and some penetration of subphase into the MMA region. Between these two concentrations the two blocks must demix, and it is tempting to relate the initial fall in relaxation time to this demixing and the concomitant decrease in transverse viscosity over the range $0 \leq \Gamma_s \leq 0.8 \text{ mg m}^{-2}$ due to increased water content of the spread film. It is in this low surface concentration region that we remarked that we always noted an increase in the static surface tension over that of the clean water surface. Such an increase in surface tension is normally attributed to a desorption from the surface. Our SQELS data also indicate that something unusual is happening in this concentration range. Firstly, the damping constants are *less* than that of the clean water, and this was always observed when experiments were repeated with fresh subphase and a newly spread block copolymer film. Furthermore we also observe this for spread films of poly(methyl methacrylate) homopolymer but *not* for spread films of poly(ethylene oxide),⁴⁴ a *graft* copolymer of the two⁴⁵ or poly(lauryl methacrylate).⁴⁶ Consequently, we do not believe that this is an artefact which may be due to instrumental broadening or

incorrect alignment. It may be due to some "ordering" of the water molecules at these low surface concentrations since there is some evidence to suggest that the spread polymer monolayer exists as islands in this range of concentrations. As the surface concentration increases the contact of the ethylene oxide segments with the water increases and eventually an apparent phase separation takes place whereby the poly(ethylene oxide) block contains a large amount of water and the poly(methyl methacrylate) block lies at the immediate air-water interface. We now have a highly complex system for which we have to describe the visco-elastic properties. In this situation it is somewhat surprising to obtain the apparently simple dependence of relaxation time on Γ_s shown in Figure 12 for $\Gamma_s > 1.0 \text{ mg m}^{-2}$ since this appears to indicate a single relaxation process. What may be happening is that the visco-elastic processes are being dominated by the PEO portion of the block copolymer since PMMA homopolymer forms a stiff condensed film which behaves as a Voigt solid.⁴⁴ As the surface concentration of the block copolymer increases, there is increased interaction between the copolymer molecules leading to an increase in the transverse shear viscosity. This argument has some support in the observation that the relaxation time observed for the dilational processes is of the same order of magnitude as that from the transverse parameters. This is sustainable if the relaxation processes are mainly attributable to the poly(ethylene oxide) portion and both relaxation processes involve the formation and destruction of loops which penetrate to a greater or lesser extent into the subphase.

Finally, we consider the question of in plane homogeneity of the spread block copolymer film. This question was discussed with reference to spread films of homopolymethyl methacrylate in an earlier paper mainly concerned with neutron reflectometry. This latter technique is relatively insensitive to in plane heterogeneities. To ascertain whether the spread film was inhomogeneous, we collected SQELS data repeatedly over an 8 h period and compared the frequencies and dampings; the q value used was 351 cm^{-1} . If the spread film was present as "islands" then these parameters should vary between those typical of a polymer covered surface and a clean water surface. No such variation was observed over the complete range of surface concentration investigated. For a different polymer, poly-lauryl methacrylate, variations in frequency have been observed.⁴⁶ Hence we conclude that for areas greater than that of the incident beam on the fluid surface, the block copolymer film is homogeneous.

Comparisons with Other Results. As remarked in the introduction, SQELS data on other polymer systems are extremely sparse. Moreover those that are available are not directly comparable to our visco-elastic parameters since these terms have either not been calculated or, where some are reported (generally ϵ_0 and ϵ'), they have been obtained assuming γ' is zero. This does not seem to be valid in all situations. Additionally the use of a simple Lorentzian to fit the data must also bias the parameters obtained, but this aspect is not too significant.

Yu and co-workers²⁹ have reported SQELS results for both poly(ethylene oxide) and poly(methyl methacrylate) homopolymer, and we can compare their damping constant values with ours. In PEO they noted a sharp maximum in damping at $\Gamma_s \sim 0.4 \text{ mg m}^{-2}$ whereas in PMMA an increase to a plateau value was observed at

$\Gamma_s \approx 0.8 \text{ mg m}^{-2}$. Our data for the block copolymer displays traces of both these features, but our absolute values of the damping constant are circa one-third of those reported by Yu et al. Dilational moduli (ϵ_0) and dilational viscosity (ϵ') for PEO spread film both went through maximum values at $\Gamma_s \approx 0.4 \text{ mg m}^{-2}$. For PMMA homopolymer the dilational modulus was large and approximately constant (with large errors) at circa 70 mN m^{-1} . The block copolymer reported here also displays maxima in both ϵ_0 and ϵ' (Figure 8), but these are located at circa $\Gamma_s \approx 1.5 \text{ mg m}^{-2}$; the absolute value of the dilational modulus is considerably higher than that of pure PEO but less than that for PMMA. On the other hand our recorded values of ϵ' are much larger than those for PEO. An additional factor is that Yu et al. obtained almost exact coincidence between dilational modulus from SQELS and the same parameter from the classical surface pressure isotherm. One is led to conclude that despite the observation of a spatial surface phase separation on increasing Γ_s , the visco-elastic behavior is not merely the sum of that for the two separate homopolymers but has distinctive features which may be unique to the copolymer architecture.

Conclusions

A linear diblock copolymer of poly(methyl methacrylate) and poly(ethylene oxide) spread at the air-water interface has been shown to demonstrate visco-elastic properties. Both transverse and dilational parameters have been extracted from the heterodyne correlation functions. Applying phenomenological models to these parameters has allowed us to calculate relaxation times. For surface concentrations above circa 1.0 mg m^{-2} , both dilational and translational relaxation times are of the same order of magnitude of circa $250 \mu\text{s}$; however, a clear concentration dependence is evident in relaxation times from the transverse visco-elastic parameters. Although frequency dependent values of the surface tension can be fitted by a Maxwell fluid model with a single relaxation time, the shape of the Cole-Cole plot of these same data suggests that there is a distribution of relaxation times. Anomalies in the surface tension data and the damping constants at low surface concentrations have been correlated with properties intrinsic to poly(methyl methacrylate) and a surface phase separation of the block copolymer observed by neutron reflectometry. The similarity of the relaxation times noted above has been attributed to the dominant role of the poly(ethylene oxide) block in determining the visco-elastic properties of the spread block copolymers; however, these properties are intrinsically different from either of the two homopolymers.

Acknowledgment. We thank the Engineering and Physical Sciences Research Council for the support of this research and the University of Durham Research Development Fund for funds which enabled the purchase of an active vibration isolation table. It is also a pleasure to thank Professor John Earnshaw of Queen's University, Belfast, for his advice, encouragement, and comment.

References and Notes

- (1) Scheutjens, J. M. H. M.; Fleer, G.; Cohen-Stuart, M.; Cosgrove, T.; Vincent, B. *Polymers at Interfaces*, Chapman and Hall: London, 1993.
- (2) Milner, S. T.; Witten, T. A.; Cates, M. E. *Macromolecules* **1988**, *21*, 2610.
- (3) Shull, K. R. *J. Chem. Phys.* **1991**, *94*, 5723.

- (4) *Faraday Discuss.* **1995**, 98. Complete issue dedicated to Polymers at Interfaces.
- (5) Field, J. B.; Toprakcioglu, C.; Ball, R. C.; Stanley, H. B.; Dai, L.; Barford, W.; Penfold, J.; Smith, G.; Hamilton, W. *Macromolecules* **1992**, 25, 434.
- (6) Cosgrove, T.; Heath, T. G.; Phipps, J. S.; Richardson, R. M. *Macromolecules* **1991**, 24, 94.
- (7) Mansfield, T. L.; Iyengar, D. R.; Beaucage, G.; McCarthy, T. J.; Stein, R. S.; Composto, R. J. *Macromolecules* **1995**, 28, 492.
- (8) Cosgrove, T.; Phipps, J.; Richardson, R. M. *Colloids Surf.* **1992**, 62, 199.
- (9) Henderson, J. A.; Richards, R. W.; Penfold, J.; Thomas, R. K. *Macromolecules* **1993**, 26, 65.
- (10) Henderson, J. A.; Richards, R. W.; Penfold, J.; Thomas, R. K.; Lu, J. *Macromolecules* **1993**, 26, 4951.
- (11) Reynolds, I.; Richards, R. W.; Webster, J. P. R. *Macromolecules* **1995**, 28, 7845.
- (12) von Smoluchowski, M. *Ann. Phys.* **1913**, 41, 609.
- (13) Kramer, L. *J. Chem. Phys.* **1971**, 55, 2097.
- (14) Levich, V. G. *Physico-Chemical Hydrodynamics*; Prentice Hall: Englewood Cliffs, NJ, 1962.
- (15) Lucassen-Reynders, E. H.; Lucassen, J. *Adv. Colloid Interface Sci.* **1969**, 2, 347.
- (16) Goodrich, F. C. *Proc. R. Soc. London A* **1961**, 260, 490.
- (17) Goodrich, F. C. *Proc. R. Soc. London A* **1981**, 374, 341.
- (18) Hård, S.; Neuman, R. D. *J. Colloid Interface Sci.* **1987**, 115, 73.
- (19) Langevin, D.; Meunier, J.; Chatenay, D. *Surfactants in Solution*; Mittal, K. L., Lindman, B., Eds.; Plenum: New York, 1984; Vol 3.
- (20) Langevin, D. *Light Scattering by Liquid Surfaces and Complementary Techniques*; Dekker: New York, 1992.
- (21) Earnshaw, J. C. In *Polymer Surfaces and Interfaces II*; Feast, W. J., Munro, H. S., Richards, R. W., Eds.; Wiley: New York, 1992; Chapter 5.
- (22) Birecki, H.; Amer, N. M. *J. Phys. (Paris) C3* **1979**, 40, 433.
- (23) Byne, D.; Earnshaw, J. C. *J. Phys. D: Appl. Phys.* **1979**, 12, 1145.
- (24) Crawford, G. E.; Earnshaw, J. C. *Biophys. J.* **1986**, 49, 869.
- (25) Earnshaw, J. C.; McCoo, E. *Langmuir* **1995**, 11, 1087.
- (26) Langevin, D. *J. Colloid Interface Sci.* **1981**, 80, 412.
- (27) Kawaguchi, M.; Sano, M.; Yen-Lane, C.; Zogafi, G.; Yu, H. *Macromolecules* **1986**, 19, 2606.
- (28) Sauer, B. B.; Yu, H.; Tien, C. F.; Hager, D. F. *Macromolecules* **1987**, 20, 393.
- (29) Kawaguchi, M.; Sauer, B. B.; Yu, H. *Macromolecules* **1989**, 22, 1735.
- (30) Earnshaw, J. C.; McGivern, R. C.; McLaughlin, A. C.; Winch, P. J. *Langmuir* **1990**, 6, 649.
- (31) Bouchiat, M. A.; Meunier, J. *J. Phys. (Paris)* **1971**, 32, 561.
- (32) May-Colaiani, S. E.; Gandhi, J. V.; Mály, K. J.; Maher, J. V.; Kuhar, K. A.; Chapman, T. M. *Macromolecules* **1993**, 26, 6595.
- (33) Richards, R. W.; Rochford, B. R.; Webster, J. P. R. *Faraday Discuss.* **1995**, 98, 263.
- (34) Rochford, B. R. Ph.D. Thesis, University of Durham, 1995.
- (35) Earnshaw, J. C.; McGivern, R. C. *J. Colloid Interface Sci.* **1988**, 123, 36.
- (36) Langevin, D. In *Light Scattering by Liquid Surfaces and Complementary Techniques*; Langevin, D., Ed.; Dekker: New York, 1992; Chapt. 6.
- (37) Jakeman, E. In *Photon Correlation and Light Beating Spectroscopy*; by Cummins, H. Z., Pike, E. R., Eds.; Plenum: New York, 1974; p 75.
- (38) Langevin, D. In *Light Scattering by Liquid Surfaces and Complementary Techniques*; ed, Langevin, D., Ed.; Dekker: New York, 1992; Chapt. 6.
- (39) Henderson, J. A. Ph.D. Thesis, University of Durham, 1992.
- (40) McCrum, N. G.; Read, B. E.; Williams, G. *Anelastic and Dielectric Effects in Polymer Solids*; Wiley: London, 1967.
- (41) Ferry, J. D. *Viscoelastic Properties of Polymers*, 3rd ed.; Wiley: New York, 1980.
- (42) Earnshaw, J. C.; McGivern, R. C.; Winch, P. J. *J. Phys. (Paris)* **1988**, 49, 1271.
- (43) Davidson, D. W.; Cole, R. H. *J. Chem. Phys.* **1950**, 18, 1417.
- (44) Taylor, M. R. Unpublished results.
- (45) Peace, S. K. Work in progress.
- (46) Reynolds, I. Work in progress.

MA950853P